Preparation of fusion materials based on ionic liquid and cationic gold nanoparticle

Takuya Nakashima,* Yu Hayakawa, Midori Mori and Tsuyoshi Kawai

Graduate School of Materials Science, Nara Institute of Science and Technology, NAIST, Nara, Japan

Correspondence: Dr. T Nakashima, Graduate School of Materials Science, Nara Institute of Science and Technology, 8916-5 Takayama, Ikoma, Nara 630-0192, Japan.

Fax: +81-743-72-6179

E-mail: ntaku@ms.naist.jp

Title Running Head: Ionic liquid-gold nanoparticle composites

Keywords: ionic liquid; gold nanoparticle; composite; self-assembly

Abstract

Fusion materials based on cationic gold nanoparticles with ionic liquids were prepared. The anion-exchange of the surface capping ligand on the gold nanoparticles from a halogen anion to bis(trifluoromethanesulfonyl)amide (Tf_2N) in an aqueous solution afforded nanoparticles showing the infinite miscibility with Tf_2N-based ionic liquids. The thermal decomposition temperature of gold nanoparticle was elevated by 100 °C after the anion-exchange. The ionic liquid-like structure of the surface capping ligand with Tf_2N anion led to a grassy solid material with densely-packed assembly of nanoparticles, in which a portion of nanoparticles formed superlattices. A fusion material of ionic liquid and gold nanoparticle with a gold content as high as 40wt% was obtained by the co-solvent evaporation method using acetone. The stable dispersion of gold nanoparticles in the fusion materials with a high gold content was confirmed by the clear appearance of the plasmon absorption of gold nanoparticles in an optical microscope image as well as in an absorption spectrum. The use of an ionic liquid-based monomer gave a gold nanoparticle-ionic liquid polymer composite, in which the gold nanoparticles showed a high thermal stability.

INTRODUCTION

Room-temperature ionic liquids (ILs) have been attracting much interest as environmentally benign solvents for organic chemical reactions, separations, and electrochemical applications.[1-5] Recent interest is focusing on their use in inorganic synthesis,[6-8] hybridization with nanomaterials,[9-11] and molecular self-assembly.[12-17] The inherent self-assembling properties of ILs themselves derived from interionic hydrogen bonding interactions[18,19] and their amphiphilic nature[20,21] most likely play an important role in the solubilization of nanomaterials including molecular self-assemblies as well as in the synthesis of nanomaterials with fine structures. ILs therefore enabled the direct *in situ* synthesis of metal nanoparticles (NPs) without addition of extra stabilizers through the chemical reduction of metal ions[22,23] and sputter depositions.[24] The reorganization of the hydrogen bond network and the generation of nanostructures of ionic components were presumed to form a protecting layer on the surface of NPs, providing both steric and electrostatic protection against agglomeration.[23] Meanwhile, the fusion of self-assembling property of ILs and functional inorganic nanomaterials is expected to lead to a futuristic material, in which both the components synergistically interact to construct a hierarchically assembled structure. Furthermore, the unique characteristics of ILs such as high ionic conductivity, thermal stability, and extremely low vapour pressure, that could be tuned by changing the anion identity and cation substituents, make them an excellent partner of nanomaterials to build composite materials together.[25-28] For example, IL-silica nanoparticle hybrids have been demonstrated as an electrolyte for batteries.[29]

A wide range of metal and semiconductor NPs with or without surface capping ligands have

been reported to be well dispersed in ILs. Since the electrostatic charge stabilization, which usually accounts for the colloidal stability of NPs in water, is considered to be insufficient owing to the high ionic strength in ionic liquids, the ionic liquid-based solvation might be responsible for the colloidal stability in ILs.[29] However, the dynamically fluctuating organized structure of ILs[20] and ill-defined interactions[30,31] between the surface of NPs and IL-components may hamper the stable dispersion of bare NPs in ionic liquids with a high NPs content especially at high temperature. In this context, NPs with imidazolium-functionalized surface capping ligands[32-34] or polymers[35] showed better stability in ILs. Some NPs stabilized by IL-based ligands showed liquid-like behavior at room temperature in the absence of solvent media.[36-38] They have conventionally been prepared in other media such as water or organic solvents, and then transferred into ILs *via* the modification of ligands. Recently we reported the spontaneous phase transfer of CdTe NPs capped with simple cationic ligands, 2-(dimethylamino)ethanethiol hydrochloride (DMAET) or thiocholine bromide (TCB), from aqueous solutions to ILs.[39-41] The cationic CdTe NPs showed remarkable stability and improved photoluminescence properties in the ILs. The use of these cationic ligands afforded the NP-IL-based polymer composites at the high volume fraction of NPs as high as 1 vol% (3.6 wt%), which demonstrated high-order optical nonlinearlities.[42,43]

In the present paper, we report the preparation of hybrid materials based on ILs with cationic gold NPs. To achieve a very high loading content of NPs in ILs, cationic NPs with bis(trifluoromethanesulfonyl)amide (Tf_2N) anion were prepared. The cationic gold NPs with Tf_2N anion formed a glassy film by cast from acetone solution and provided fusion materials with ILs at

the content of gold as high as 40wt%. The gold NPs exhibited a high thermal stability in an IL-based polymer.

EXPERIMENTAL PROCEDURE

Materials and methods

1-Butyl-3-methylimidazolium bis(trifluoromethanesulfonyl)amide (bmimTf_2N) and lithium bis(trifluoromethanesulfonyl)amide ($LiTf_2N$) were purchased from Kanto Chemical Co., Inc. 2-(Methacryloyloxy)ethyltrimethylammonium bis(trifluoromethanesulfonyl)amide (MOE-200) was purchased from Piotrek Co., Ltd. 2-(Dimethylamino)ethanethiol hydrochloride (DMAET) was obtained from Sigma-Aldrich. Hydrogen tetrachloroaurate(III) tetrahydrate ($HAuCl_4 \cdot 4H_2O$) was supplied by Wako Pure Chemical Industries Ltd. Irgacure 184 (1-hydroxycyclohexyl phenyl ketone) was obtained from TCI Co. Ltd. These chemicals were used as received. Diethylene glycol dimethacrylate (DEGDMA) was obtained from TCI Co. Ltd. and used after a simple distillation process. Absorption spectra in solution were studied with a JASCO V-670 spectrophotometer. Thermogravimetric analysis (TGA) was carried out using a TG-DTA6200 (SII Technology). Transmission electron microscopy (TEM) observation was performed with a JEM-2200FS (JEOL). Scanning electron micrographs (SEM) were obtained by using an SU9000 (Hitachi). Small angle X-ray scattering (SAXS) profile was recorded using a Rigaku RINT-TTR III/NM X-ray diffractometer in transmission mode. Absorption spectra of concentrated fusion materials were

measured by using an Olympus BX-51 polarizing microscope connected with a Hamamatsu PMA-11 photodetector with an optical fiber.

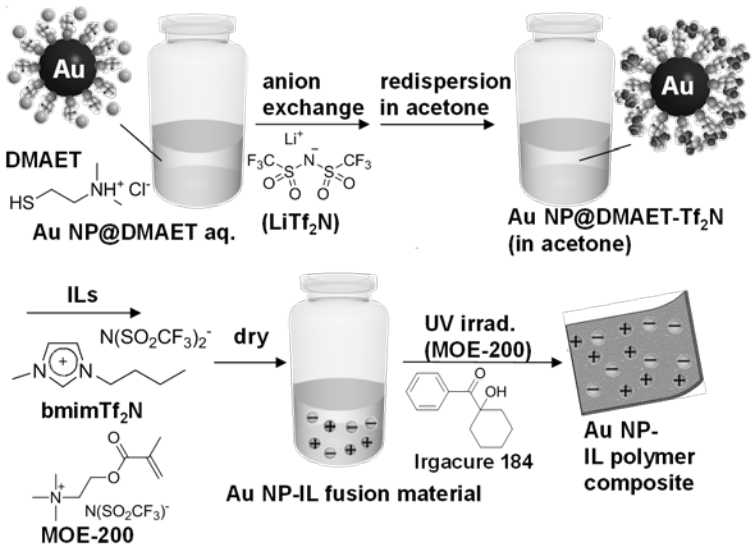

Scheme 1 Preparation of fusion materials based on gold NPs and ILs.

Synthesis of DMAET capped gold NPs and fusion materials: Fusion materials based on gold nanoparticles and ILs were prepared according to Scheme 1. The gold NPs were synthesized by the chemical reduction of Au^{3+} in an aqueous solution in the presence of cationic thiol DMAET. To a solution of $HAuCl_4 \cdot 4H_2O$ (0.33 g, 0.80 mmol) and DMAET (0.28 g, 2.4 mmol) in deionized water (67 ml) an aqueous solution (6.7 ml) of sodium borohydride ($NaBH_4$) (20 mg, 0.53 mmol) was added under vigorous stirring in an ice bath. After stirred for 1 h, the insoluble sediment was removed through centrifugation followed by decantation. DMAET capped gold NPs in the supernatant was purified *via* reprecipitation by the addition of acetone (300 ml). The precipitation was freeze-dried to give 82 mg of the DMAET-capped gold NPs in 44% yield (in terms of the

conversion of Au^{3+}). 50 mg of the DMAET-capped gold NPs were redispersed in deionized water (10 ml), to which an aqueous solution of $LiTf_2N$ (70 mg, 0.24 mmol) was added to exchange the counter anion of DMAET from Cl^- to Tf_2N^-. DMAET-Tf_2N passivated gold NPs was then obtained as a precipitate. The precipitated gold NPs were freeze-dried by a lyophilizer to give 46 mg of cottony powder in 61% yield.

The DMAET-Tf_2N passivated gold NPs were dispersed in acetone with a certain amount of ILs ($bmimTf_2N$ or MOE-200, Scheme 1). The fusion materials were obtained after the evaporation of acetone in vacuo. The fusion material of MOE-200 was further polymerized by photoradical polymerization. To a mixture of gold NPs and MOE-200, a cross linker DEGDMA (20wt%) and an acetone solution of Irgacure 184 (1wt%) were added, acetone was evaporated in vacuo and then the mixture was degassed. The monomer cocktail was cast on a glass substrate loaded with a silicone film spacer (thickness: 100 μm) and was covered with another glass substrate. The photopolymerizable nanocomposite film was exposed by UV light with a mercury-xenon lamp (200W) through a UV transmitting filter at room temperature to prepare a uniformly cured polymer nanocomposite film.

RESULTS AND DISCUSSION

DMAET-Tf_2N-capped gold NPs

Figure 1 shows TEM image of DMAET protected gold NPs before anion-exchange prepared from an aqueous solution. Relatively monodisperse quasi-spherical NPs with the average diameter

of 2.9 ± 0.4 nm were observed. In the absorption spectrum, an apparent plasmon absorption peak appeared at 517 nm (Figure 2). The anion exchange of the gold NPs from chloride to Tf_2N made the NPs insoluble in water but soluble in high polar organic solvents such as acetone. The hydrophilic chloride anion is supposed to tightly bind to the ammonium cation of DMAET and form aggregates in acetone, which was demonstrated by the precipitation purification procedure of DMAET-capped gold NPs using acetone. The anion exchange to Tf_2N with a higher ionic radius decreased the hydrophilicity of the counter anion, which was expected to reduce the interionic interaction and allowed ions to partially dissociate in acetone.[44] The DMAET-Tf_2N passivated gold NPs also exhibited a clear plasmon absorption peak in acetone, suggesting the stable dispersion of NPs. The peak appeared at 510 nm, which was slightly shorter than that observed in water probably due to the change in the permittivity of solvents.[45]

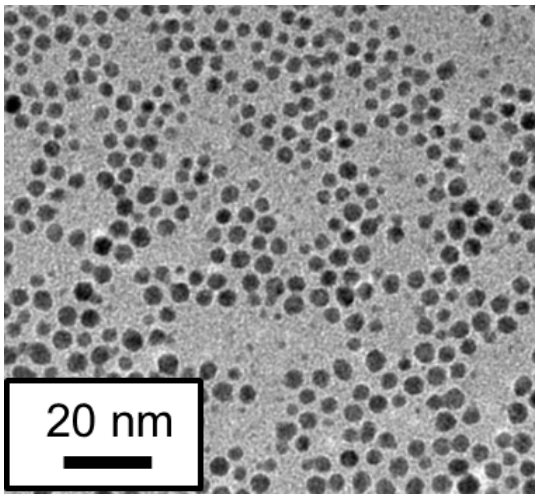

Figure 1 TEM image of DMAET capped gold NPs cast from an aqueous solution.

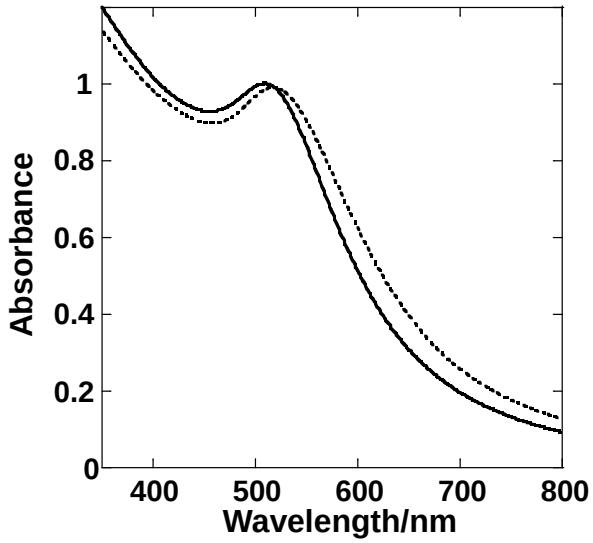

Figure 2 Absorption spectra of DMAET capped gold NPs in water (dotted line) and in acetone (solid line) after the anion exchange with Tf_2N.

The acetone solution of gold NPs was cast on a TEM grid, which was observed by TEM and SEM. As shown in Figure 3a, the gold NPs formed a densely packed glassy-assembled film on the TEM grid. The separation between NPs was apparently shorter than that observed for the TEM image in Figure 1. Since the thickness of an electrical double layer (EDL) is dependent on the permittivity of solvents,[46] the reduced electrostatic repulsion in the acetone was responsible for the densely packed assembly. Larger particles with the size of a few hundred nanometers were also observed on the glassy amorphous film as shown in Figure 3b (SEM). Interestingly, the large particles were recognized as the secondary particles composed of the individual cationic gold NPs assembling into superlattice structures, which were confirmed by a high-resolution SEM image (Figure 3c). These super-crystalline structures could be formed during the evaporation since the acetone solution for EM measurements was subjected to centrifugation with 10^4 rpm followed by

filtration with a membrane filter prior to the drop-cast. The elevation of NP concentration and ionic strength during the evaporation of solvent may result in the close contact between NPs by minimizing the EDL so that the *van der Waals* force between NPs became effective.[46] Furthermore, the cohesive interactions between IL-like DMAET-Tf_2N surface ligands, which could give rise to the self-assembling property of ILs, should play a crucial role in the self-assembly of NPs.

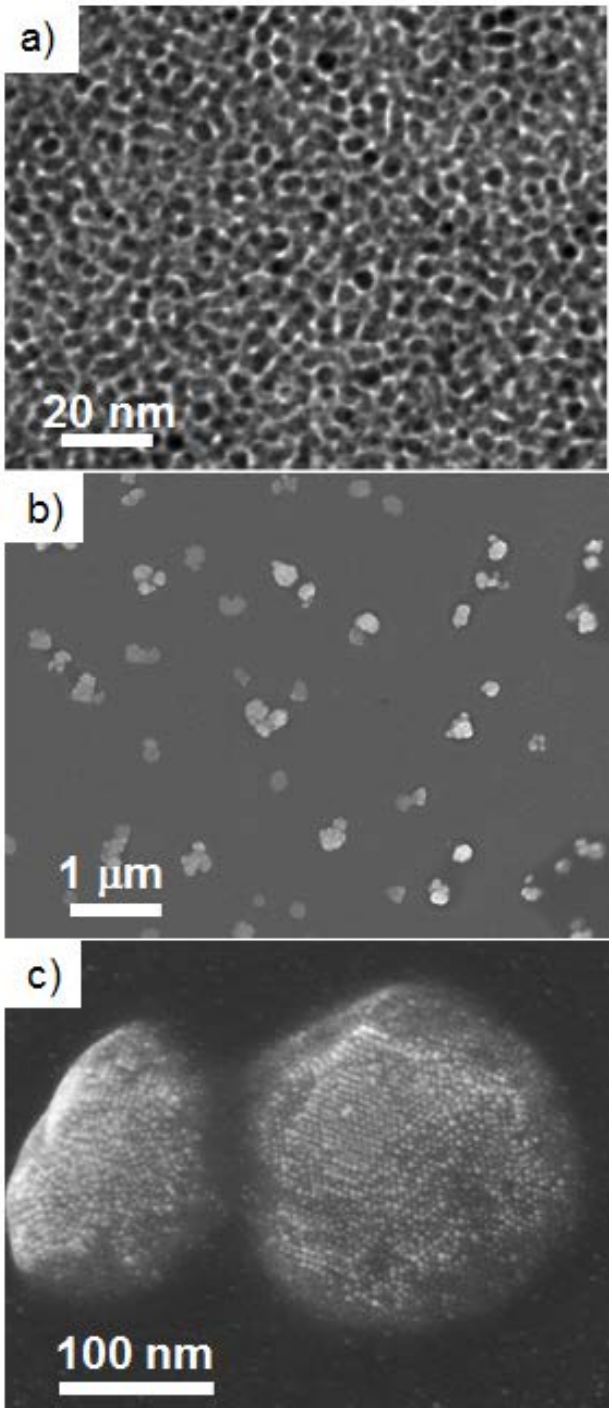

Figure 3 Electron micrographs of DMAET-Tf_2N capped gold NPs prepared from an acetone solution: a) TEM, b), c) SEM images.

The properties of DMAET-Tf_2N capped gold NPs in bulk were also investigated by thermal analytical methods. The DMAET-capped NPs before the anion exchange decomposed at around

200 °C probably because of the high chemical reactivity of chloride anion (Figure 4). The anion exchange to Tf_2N elevated the decomposition temperature of ligands. The mass decrease of DMAET-Tf_2N capped gold NP started from about 300 °C, which was higher than that of the gold NPs before anion exchange by 100 °C, directly indicating the higher chemical stability of Tf_2N^- in comparison to Cl^-. The DMAET capped gold NPs contained the organic content by 29wt%, corresponding to 430 ligand molecules per single NP (6.1 $Å^2$ of occupied surface area per a ligand molecule). This number seems too large considering that the typical occupied surface area of a similar ligand molecule TCB was estimated to be 22.9 $Å^2$,[47] indicating the presence of unbound excess ligand molecules. Similarly, the DMAET-Tf_2N capped gold NPs possessed a 42wt% portion of organic ligands, which corresponds to 280 ligand molecules per single NP and still had unbound excess ligand molecules.

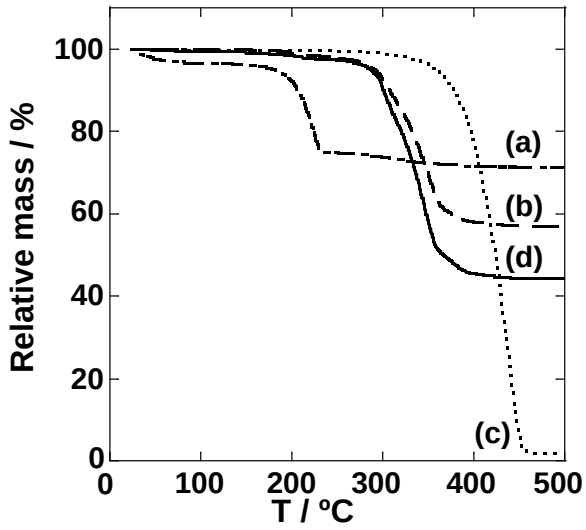

Figure 4 Thermogravimetric curves of (a) DMAET-capped gold NP, (b) DMAET-Tf_2N capped gold NP, (c) bmimTf_2N and (d) gold NP-bmimTf_2N composite.

Figure 5 shows DSC thermograms of DMAET-Tf_2N and gold NPs. DMAET-Tf_2N became an ionic liquid after the anion exchange. The free DMAET-Tf_2N showed an exothermic peak at -47 °C corresponding to the cold-crystallization and endothermic peaks at -7 and 7 °C assigned to melting points, which were typical to Tf_2N-based ILs.[48] On the other hand, the DMAET-Tf_2N capped gold NPs showed no apparent DSC peak, indicating the free excess DMAET-Tf_2N ligands had a negligible effect on the thermal behavior of NPs. The DSC profile of the gold NPs exhibited a slight endothermic shift of the baseline at 58 °C corresponding to the glass transition temperature, which also supported the glassy amorphous assembly of gold NPs in the solid state. There is no endothermic peak observed for the melting of superlattice assemblies in the range of temperature investigated, indicating the supercrystallines were only the minor components in the solid film. The SAXS profile measured for the DMAET-Tf_2N capped gold NPs suggested the amorphous-like assembly in the cast film, which provided a broad peak corresponding to the interparticle correlation with distance of 4.8 nm and gave little indication of highly ordered aggregation with periodic peaks (Figure S1).

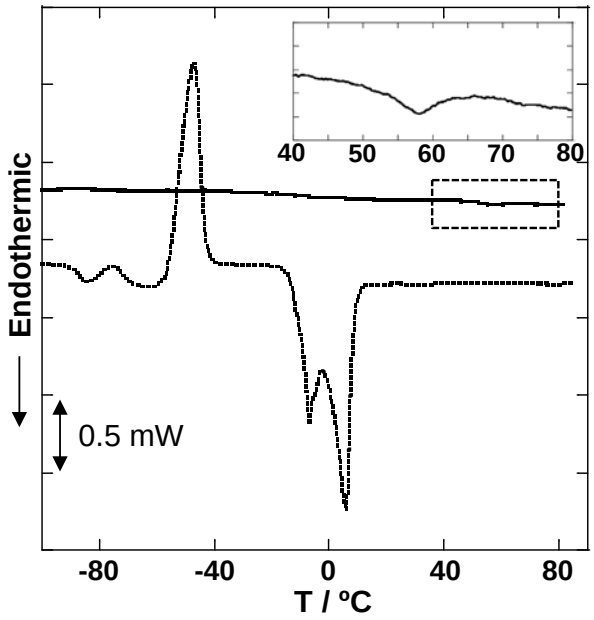

Figure 5 DSC thermograms of DMAET-Tf_2N (dotted line) and DMAET-Tf_2N-capped gold NPs (solid line). Inset: enlarged profile of DMAET-Tf_2N-caped gold NPs.

Fusion materials of DMAET-Tf_2N-capped gold NPs and ILs.

The DMAET-Tf_2N capped gold NPs were mixed with bmimTf_2N by a co-solvent evaporation method using acetone, since the direct dispersion of NPs resulted in the partial solubilization of NPs in ILs due to the high viscosity of ionic liquids. BmimTf_2N was thermally stable up to 350 °C (Figure 4c), while the concentrated composite with a 40wt% of gold content showed the decomposition above 300 °C (Figure 4d). The decomposition temperature of the composite was identical with that of DMAET-Tf_2N capped gold NPs without IL (Figure 4b), which indicated that the decomposition started from the NPs in the composite.

The gold NPs were homogeneously dispersed in bmimTf_2N in a given composition after the evaporation of acetone. Figure 6a shows a visual appearance of the NP-bmimTf_2N composite with

a gold content of 40wt%. Although the composite was black and highly sticky paste in bulk, it actually appeared in red in a thin film wedged between glass slides (Figure 6b). The red color originates from the plasmon absorption (Figure 6c) of individual NPs in the composite, which clearly suggested the NPs were well dispersed in bmimTf_2N even at high concentration. The value of 40wt% as a gold content corresponds to 5vol% of a volume fraction of gold, in which the average inter-NP distance can be estimated to be 6.3 nm given a random dispersion. The distance of 6.3 nm might not be close enough to observe the plasmonic coupling between NPs,[49] and no apparent peak shift was found in the peak position of absorption spectrum in comparison with that of dilute solution in acetone (Figure 6b and Figure 1).

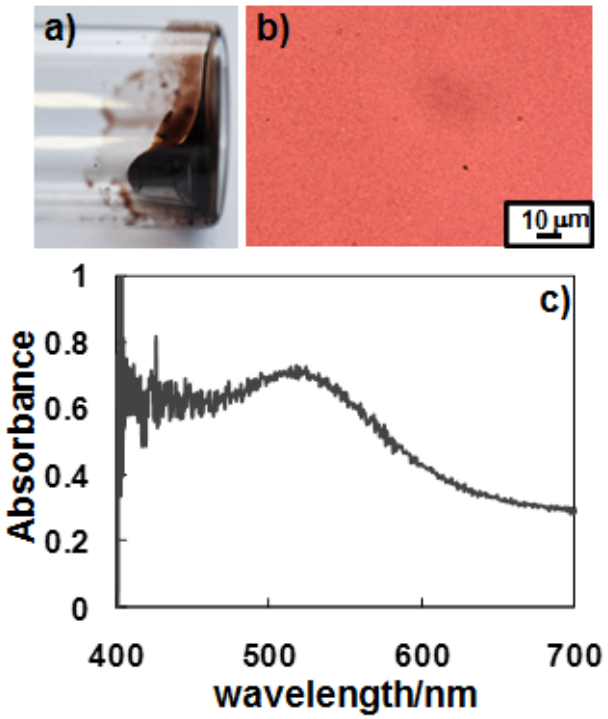

Figure 6 (a) Photograph and (b) optical microscope image of gold NP-bmimTf_2N composite (Au content = 40wt%) and (c) its absorption spectrum.

The composite of NP-bmimTf_2N was directly observed by TEM. Since the composite was highly sticky, the sample for TEM was prepared by diluting the composite with a small amount of acetone followed by casting the methanol solution on a TEM grid. A certain amount of bmimTf_2N remained on the TEM grid together with the gold NPs because bmimTf_2N was difficult to evaporate. It should be noted that the composition ratio between the NPs and bmimTf_2N was not preserved because acetone could rinse off part of bmimTf_2N. As shown in Figure 7, the gold NPs appeared to aggregate in the droplets of bmimTf_2N as the slightly dark background of aggregates.[50] The aggregate structures of the composite was very different from those obtained for the sample without bmimTf_2N (Figure 3). The gold NPs formed no supercrystals but irregularly assembled into lumps. The individual NPs were identified in the aggregates, corresponding to the appearance of plasmon absorption band for the composite (Figure 6). ILs were reported to form the double-layer at a charged surface,[51] which was also expected to induce the layering of ionic components in an alternate manner.[28,52] The layering of ionic components was estimated to extend to ten-bilayers.[53] The cationic gold NPs were therefore expected to be strongly solvated by the formation of multilayer of ionic components triggered by the ordering of Tf_2N anions at the interface, which might also hinder the tightly packing of NPs into superlattices *via van der Waals* interactions between the NPs.

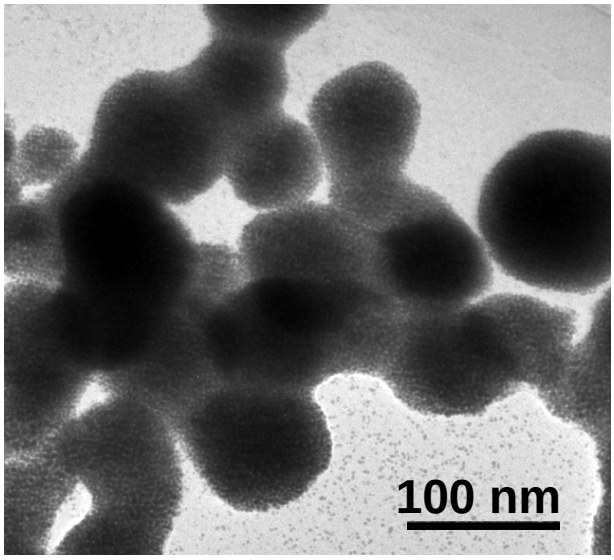

Figure 7 Typical TEM image of gold-NP-bmimTf_2N composite.

The DMAET-Tf_2N capped gold NPs were also well dispersed in a polymerizable IL, MOE-200. The NP-monomer composite was then mixed with a photoinitiator, Irgacure 184, and a cross-linker, DEGDMA, followed by irradiated with UV light to give a polymer composite film of NPs with a thickness of 100 μm. The polymer composite was basically transparent and colored in brown with the clear appearance of plasmon absorption of individual NPs (Figure 8), suggesting the good dispersion of NPs in the ionic liquid polymer. The increase in the gold content decreases the transmittance of composite film due to the high optical density of plasmon absorption. The TG analysis of polymer-composite suggested the film could incorporate the gold as high as 13wt% (Figure S2). While we also tried to prepare the composite film with the gold content of 20wt%, the high optical density of the film prevented the photopolymerization of entire film. The gold NPs showed high thermal stability in the polymer. The heat treatment of the monomer solution at 100 °C for 10 min resulted in the irreversible agglomeration of NPs (Figure S3) and the monomeric

composite became opaque with the disappearance of plasmon absorption band characteristic to gold NPs (Figure 8b). Although the thermal decomposition of the ligand of NPs started above 300 °C (Figure 4), the heating might activate the diffusion collision of NPs and the desorption of surface ligands, which induced the thermal fusion of gold NPs. On the other hand, the heating of the polymeric composite led to only slight change in the absorption spectrum even annealed at 230 °C for 30 min (Figure 8a). The suppressed diffusion of NPs immobilized in the solid matrix and the thermal stability of IL-polymer would be responsible for the stability of NPs in the composite.

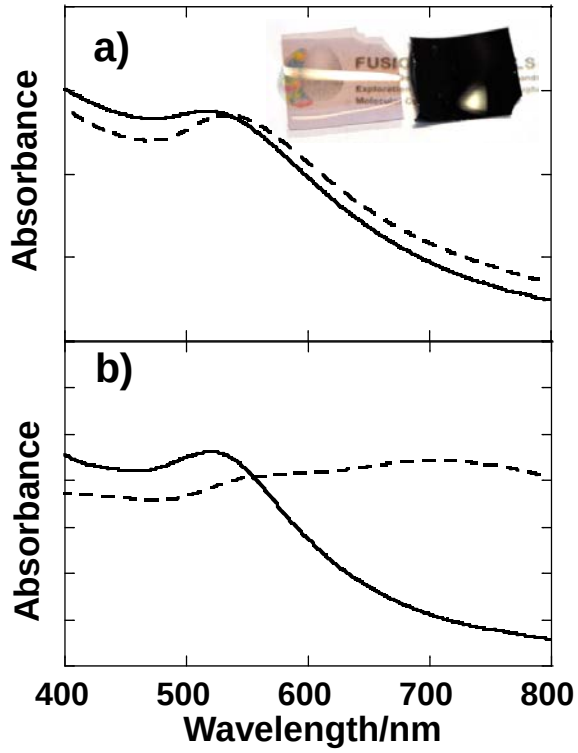

Figure 8 Absorption spectra of gold NPs in polymer(a) and monomer (b) before (solid lines) and after (broken lines) the heat treatment. Inset: picture of the polymer composite films with different gold content.

CONCLUSION

In conclusion, gold NPs capped with a simplified IL-like ligand were prepared, which were incorporated into fusion materials with ionic liquids. The high cohesive energy of IL-like ligand drove the assembly of NPs into a glassy amorphous film and superlattices. The DMAET-Tf_2N capped gold NPs were well dispersed in Tf_2N-based ILs with high concentration up to a 40wt% of inorganic content. The fusion material of gold NPs with an ionic liquid monomer was readily converted into a polymeric composite, in which gold NPs showed high thermal stability. We envisage the IL-like ligand with a simple structure could be a universal ligand for a wide range of inorganic nanoparticles to provide an interface compatible with ILs.

ACKNOWLEDGEMENTS

This work was supported in part by a Grant-in-Aid for Scientific Research on Innovative Areas of “Fusion Materials” (Area no. 2206) from the Ministry of Education, Culture, Sports, Science and Technology (MEXT).

References

1. Parvulescu, V. I. & Hardacre, C. Catalysis in ionic liquids. *Chem. Rev.* **107**, 2615-2665 (2007).
2. Han, X. & Armstrong, D. W. Ionic liquids in separations. *Acc. Chem. Res.* **40**, 1079-1086 (2007).
3. MacFarlane, D. R., Pringle, J. M., Howlett, P. C. & Forsyth, M. Ionic liquids and reactions at the electrochemical interface. *Phys. Chem. Chem. Phys.* **12**, 1659-1669 (2010).
4. Armand, M., Endres, F., MacFarlane, D. R., Ohno, H. & Scrosati, B. Ionic-liquid materials for the electrochemical challenges of the future. *Nat. Mater.* **8**, 621-629 (2009).
5. Smiglak, M., Pringle, J. M., Lu, X., Han, L., Zhang, S., Gao, H., MacFarlane, D. R. & Rogers, R. D. Ionic liquids for energy, materials, and medicine. *Chem. Commun.* **50**, 9228-9250 (2014).
6. Nakashima, T. & Kimizuka, N. Interfacial synthesis of hollow TiO_2 microspheres in ionic liquids. *J. Am. Chem. Soc.* **125**, 6386-6387 (2003).
7. Antonietti, M., Kuang, D. B., Smarsly, B. & Yong, Z. Ionic liquids for the convenient synthesis of functional nanoparticles and other inorganic nanostructures. *Angew. Chem.-Int. Edit.* **43**, 4988-4992 (2004).
8. Ma, Z., Yu, J. H. & Dai, S. Preparation of inorganic materials using ionic liquids. *Adv. Mater.* **22**, 261-285 (2010).
9. Torimoto, T., Tsuda, T., Okazaki, K. & Kuwabata, S. New frontiers in materials science opened by ionic liquids. *Adv. Mater.* **22**, 1196-1221 (2010).
10. Fukushima, T., Kosaka, A., Ishimura, Y., Yamamoto, T., Takigawa, N., Ishii, N. & Aida, T. Molecular ordering of organic molten salts triggered by single-walled carbon nanotubes. *Science* **300**, 2072-2074 (2003).
11. Dupont, J. From molten salts to ionic liquids: a "nano" journey. *Acc. Chem. Res.* **44**, 1223-1231 (2011).
12. Kato, T. Self-assembly of phase-segregated liquid crystal structures. *Science* **295**, 2414-2418 (2002).
13. Greaves, T. L. & Drummond, C. J. Ionic liquids as amphiphile self-assembly media. *Chem. Soc.*

Rev. **37**, 1709-1726 (2008).

14. Kimizuka, N. & Nakashima, T. Spontaneous self-assembly of glycolipid bilayer membranes in sugar-philic ionic liquids and formation of ionogels. *Langmuir* **17**, 6759-6761 (2001).
15. Nakashima, T., Zhu, J., Qin, M., Ho, S.-S., Kotov, N. A. Polyelectrolyte and carbon nanotube multilayers made from ionic liquid solutions. *Nanoscale* **2**, 2084-2090 (2010).
16. Nakashima, T., Kimizuka, N. Water/Ionic liquid interfaces as fluid scaffolds for the two-dimensional self-assembly of charged nanospheres. *Langmuir* **27**, 1281-1285 (2011).
17. Nakashima, T. & Kimizuka, N. Controlled self-assembly of amphiphiles in ionic liquids and the formation of ionogels by molecular tuning of cohesive energies. *Polym. J.* 44, 665-671 (2012).
18. Fumino, K., Wulf, A. & Ludwig, R. Strong, localized, and directional hydrogen bonds fluidize ionic liquids. *Angew. Chem. Int. Ed.* **47**, 8731-8734 (2008).
19. Choudhury, A. R., Winterton, N., Steiner, A., Cooper, A. I. & Johnson, K. A. In situ crystallization of ionic liquids with melting points below 25 °C. *CrystEngComm* **8**, 742-745 (2006).
20. Lopes, J. & Padua, A. A. H. Nanostructural organization in ionic liquids. *J. Phys. Chem. B* **110**, 3330-3335 (2006).
21. Triolo, A., Russina, O., Bleif, H. J. & Di Cola, E. Nanoscale segregation in room temperature ionic liquids. *J. Phys. Chem. B* **111**, 4641-4644 (2007).
22. Scholten, J. D., Leal, B. C. & Dupont, J. Transition metal nanoparticle catalysis in ionic liquids. *ACS Catalysis* **2**, 184-200 (2012).
23. Dupont, J. & Scholten, J. D. On the structural and surface properties of transition-metal nanoparticles in ionic liquids. *Chem. Soc. Rev.* **39**, 1780-1804 (2010).
24. Torimoto, T., Okazaki, K., Kiyama, T., Hirahara, K., Tanaka, N., Kuwabata, S. Sputter deposition onto ionic liquids: Simple and clean synthesis of highly dispersed ultrafine metal nanoparticles. *Appl. Phys. Lett.* **89**, 243117-1–243117-3 (2006).
25. Le Bideau, J., Viau, L. & Vioux, A. Ionogels, ionic liquid based hybrid materials. *Chem. Soc.*

Rev. **40**, 907-925 (2011).

26. Fukushima, T. & Aida, T. Ionic liquids for soft functional materials with carbon nanotubes. *Chem. Eur. J.* **13**, 5048-5058 (2007).
27. Bara, J. E., Camper, D. E., Gin, D. L. & Noble, R. D. Room-temperature ionic liquids and composite materials: Platform technologies for CO_2 capture. *Acc. Chem. Res.* **43**, 152-159 (2010).
28. Ueno, K. & Watanabe, M. From colloidal stability in ionic liquids to advanced soft materials using unique media. *Langmuir* **27**, 9105-9115 (2011).
29. Lu, Y., Das, S. K., Moganty, S. S. & Archer, L. A. Ionic liquid-nanoparticle hybrid electrolytes and their application in secondary lithium-metal batteries. *Adv. Mater.* **24**, 4430-4435 (2012).
30. Bernardi, F. Scholten, J. D. Fecher, G. H. Dupont, J. & Morais, J. Probing the chemical interaction between iridium nanoparticles and ionic liquid by XPS analysis. *Chem. Phys. Lett.* **479**, 113−116 (2009).
31. Kauling, A., Ebeling, G., Morais, J., Padua, A., Grehl, T., Brongersma, H. H. & Dupont, J. Surface composition/organization of ionic liquids with au nanoparticles revealed by high-sensitivity low-energy ion scattering. *Langmuir* **29**, 14301-14306 (2013).
32. Itoh, H., Naka, K. & Chujo, Y. Synthesis of gold nanoparticles modified with ionic liquid based on the imidazolium cation. *J. Am. Chem. Soc.* **126**, 3026-3027 (2004).
33. Tatumi, R. & Fujihara, H. Remarkably stable gold nanoparticles functionalized with a zwitterionic liquid based on imidazolium sulfonate in a high concentration of aqueous electrolyte and ionic liquid. *Chem. Commun.* 83-85 (2005).
34. Moganty, S. S., Srivastava, S., Lu, Y., Schaefer, J. L., Rizvi, S. A. & Archer, L. A. Ionic liquid-tethered nanoparticle suspensions: A novel class of ionogels. *Chem. Mater.* **24**, 1386-1392 (2012).
35. Ueno, K., Sano, Y., Inaba, A., Kondoh, M. & Watanabe, M. Soft glassy colloidal arrays in an ionic liquid: Colloidal glass transition, ionic transport, and structural color in relation to

microstructure. *J. Phys. Chem. B* **114**, 13095-13103 (2010).

36. Bourlinos, A. B., Herrera, R., Chalkias, N., Jiang, D. D., Zhang, Q., Archer, L. A. & Giannelis, E. P. Surface-functionalized nanoparticles with liquid-like behavior. *Adv. Mater.* **17**, 234-237 (2005).
37. Warren, S. C., Banholzer, M. J., Slaughter, L. S., Giannelis, E. P., DiSalvo, F. J. & Wiesner, U. B. Generalized route to metal nanoparticles with liquid behavior. *J. Am. Chem. Soc. 128*, 12074-12075 (2006).
38. Kim, Y., Kim, D., Kwon, I., Jung, H. W. & Cho, J. Solvent-free nanoparticle fluids with highly collective functionalities for layer-by-layer assembly. *J. Mater. Chem.* **22**, 11488-11493 (2012).
39. Nakashima, T. & Kawai, T. Quantum dots-ionic liquid hybrids: Efficient extraction of cationic CdTe nanocrystals into an ionic liquid. *Chem. Commun.* 1643-1645 (2005).
40. Nakashima, T., Sakakibara, T. & Kawai, T. Highly luminescent CdTe nanocrystal-polymer composites based on ionic liquid. *Chem. Lett.* **34**, 1410-1411 (2005).
41. Nakashima, T., Nonoguchi, Y. & Kawai, T. Ionic liquid-based luminescent composite materials. *Polym. Adv. Technol.* **19**, 1401-1405 (2008).
42. Liu, X. M., Tomita, Y., Oshima, J., Chikama, K., Matsubara, K., Nakashima, T. & Kawai, T. Holographic assembly of semiconductor cdse quantum dots in polymer for volume Bragg grating structures with diffraction efficiency near 100%. *Appl. Phys. Lett.* **95**, 261109 (2009).
43. Liu, X. M., Adachi, Y., Tomita, Y., Oshima, J., Nakashima, T. & Kawai, T. High-order nonlinear optical response of a polymer nanocomposite film incorporating semiconducotor CdSe quantum dots. *Opt. Express* **20**, 13457-13469 (2012).
44. Ono, T., Ohta, M. & Sada, K. Ionic polymers act as polyelectrolytes in nonpolar media. *ACS Macro Lett.* **1**, 1270-1273 (2012).
45. Templeton, A. C., Pietron, J. J., Murray, R. W. & Mulvaney, P. Solvent refractive index and core charge influences on the surface plasmon absorbance of alkanethiolate monolayer-protected gold clusters. *J. Phys. Chem. B* **104**, 564-570 (2000).

46. Israelachvili, J. *Intermolecular and Surface Forces* 2nd edn (Academic Press, San Diego, CA, USA 1991).

47. Yonezawa, T., Onoue, S.-i. & Kimizuka, N. Metal coating of DNA molecules by cationic, metastable gold nanoparticles. *Chem. Lett.* 1172-1173 (2002).

48. Fredlake, C. P., Crosthwaite, J. M., Hert, D. G., Aki, S. N. V. K. & Brennecke, J. F. *J. Chem. Eng. Data* **49**, 49, 954-964 (2004).

49. Zhong, Z., Patskovskyy, S., Bouvrette, P., Luong, J. H. T. & Gedanken, A. The surface chemistry of Au colloids and their interactions with functional amino acids. *J. Phys. Chem. B* **108**, 4046-4052 (2004).

50. Ueno, K., Inaba, A., Kondoh, M. & Watanabe, M. Colloidal stability of bare and polymer-grafted silica nanoparticles in ionic liquids. *Langmuir* **24**, 5253-5259 (2008).

51. Sha, M., Wu, G., Dou, Q., Tang, Z. & Fang, H. Double-layer formation of [Bmim][Pf_6] ionic liquid triggered by surface negative charge. *Langmuir* **26**, 12667-12672 (2010).

52. Hayes, R., Warr, G. G. & Atkin, R. At the interface: Solvation and designing ionic liquids. *Phys. Chem. Chem. Phys.* **12**, 1709-1723 (2010).

53. Ueno, K., Kasuya, M., Watanabe, M., Mizukami, M. & Kurihara, K. Resonance shear measurement of nanoconfined ionic liquids. *Phys. Chem. Chem. Phys.* **12**, 4066-4071 (2010).

GAPHICAL ABSTRACT